

Synchronous Emission from Nanometric Silver Particles through Plasmonic Coupling on Silver Nanowires

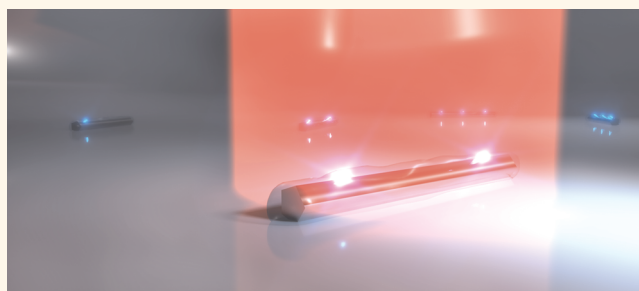
Melari Davies,^{†,§} Angela Wochnik,^{†,§} Florian Feil,^{†,§} Christophe Jung,[‡] Christoph Bräuchle,[†] Christina Scheu,^{†,*} and Jens Michaelis^{†,*}

[†]Department of Chemistry and Center for Nano Science (CeNS), Ludwig-Maximilians-University Munich, Butenandtstr. 11, 81377 Munich, Germany and [‡]Department of Biochemistry, Ludwig-Maximilians-University Munich, Feodor-Lynenstr. 25, 81377 Munich, Germany. [§]These authors contributed equally to this work. [⊥]Present address: Institute for Experimental Biophysics, Physics Department, Ulm University, Albert-Einstein-Allee 11, 89081 Ulm, Germany.

In recent years, there has been a growing interest in the synthesis and control of nanostructures of (noble) metal assemblies. Their unique optical properties caused by the collective oscillation of free electrons, known as plasmon resonances, are a central subject of most recent research.^{1–3} In particular, silver is known for exhibiting plasmon resonances for particle sizes in the nanometer regime. Also the shape of the metal, such as the aspect ratio of silver nanowires, has a tremendous influence on the plasmonic properties.⁴ Consequently, a thorough understanding of these properties is essential for the development of customized plasmonic systems for nanotechnology applications. Such potential utilizations include surface-enhanced Raman scattering (SERS),^{5–8} plasmon wave-guiding,^{9–13} gas or biomolecular sensors,^{14,15} and coupling to luminescent particles, such as dye molecules,^{16–18} quantum dots,^{19,20} or metal nanoparticles.²¹ Despite the extensive efforts put into the investigation of synthesis conditions of metal nanoparticles, such as silver nanowires (Ag-NWs), and their plasmonic properties for spectroscopic enhancement, only few studies on their luminescence after photoactivation exist as high detection sensitivity is required.^{22–24}

Uniform silver nanowires are usually synthesized by templating methods using either hard templates, such as porous alumina,²⁵ or soft templates, including cetyltrimethylammonium bromide (CTAB),²⁶ polyvinylpyrrolidone (PVP),^{27,28} or trisodium citrate.²⁹ It is known that small defects in the nanowire as well as the presence of silver nanoparticles in the close vicinity of the nanowire can have tremendous influence on their emission properties. One important example is the photochemical formation of

ABSTRACT



We investigated silver nanowires using correlative wide-field fluorescence and transmission electron microscopy. In the wide-field fluorescence images, synchronous emission from different distinct positions along the silver nanowires was observed. The sites of emission were separated spatially by up to several micrometers. Nanowires emitting in such cooperative manner were then also investigated with a combination of transmission electron microscopy based techniques, such as high-resolution, bright-field imaging, electron diffraction, high-angle annular dark-field imaging, and energy-dispersive X-ray spectroscopy. In particular, analyzing the chemical composition of the emissive areas using energy-dispersive X-ray spectroscopy led to the model that the active emissive centers are small silver clusters generated photochemically and that individual clusters are coupled *via* surface plasmons of the nanowire.

KEYWORDS: silver nanowire · plasmon coupling · synchronous fluorescence emission · single molecule fluorescence · HR-TEM

a silver nanocluster in such defects, which form local emitting entities. The formation of such entities has recently been described.^{30–33} First, pure silver is oxidized, followed by the generation of small silver clusters within the silver oxide layer caused by irradiation with a laser beam.

Important insight into the emission characteristics of metal nanoparticles can be obtained by single molecule spectroscopy (SMS) experiments, where a single particle or molecule is observed continuously over a long time interval, providing a direct view

* Address correspondence to
jens.michaelis@uni-ulm.de,
christina.scheu@cup.uni-muenchen.de.

Received for review March 14, 2012
and accepted June 4, 2012.

Published online
10.1021/nn3011224

© XXXX American Chemical Society

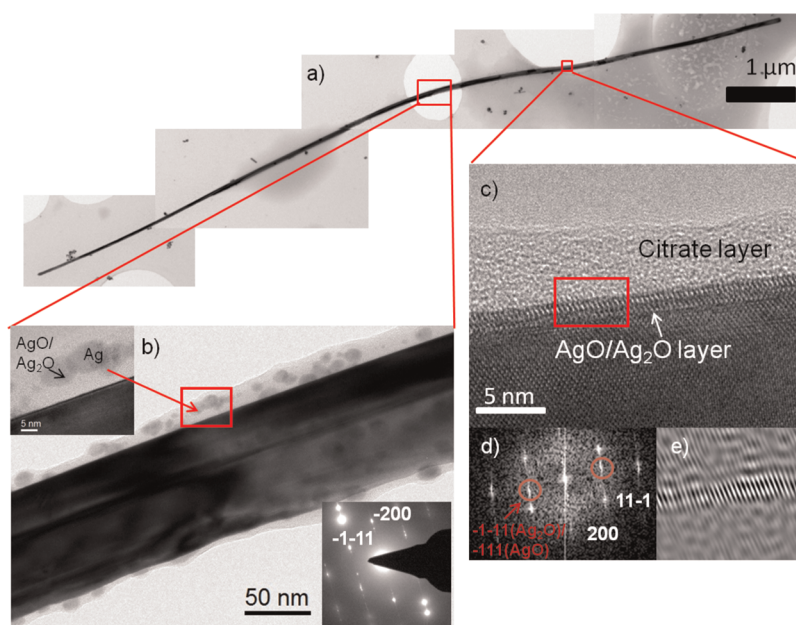


Figure 1. (a) Bright-field TEM image of an exemplary silver nanowire with dimensions of about 11 μm length and 80 nm thickness. The red squares indicate specific areas that were then imaged at higher magnifications. (b) Higher magnified TEM image of a selected area showing a 10–20 nm thick layer surrounding the Ag-NW, which was attributed to citrate. The inset in the top left shows the Ag-NW surface at even higher magnification. In the citrate layer, particles of about 5–10 nm can be observed, which are attributed to AgO, Ag₂O, or Ag. The recorded electron diffraction pattern of the Ag-NW indicates the presence of pure Ag (second inset). (c) High-resolution image of a specific region from (a) showing the citrate layer surrounding the Ag-NW and an additionally 2–3 nm thick layer on the interface between the NW and citrate layer. (d) Fast Fourier transformation of the marked area (red) in (c) shows an [011] orientation of the nanowire and indicates reflections corresponding to the d values of Ag. One additional set of reflections (red) was found, which matches the $(-1-11)$ plane of Ag₂O or (-111) of AgO. (e) Inverse fast Fourier transformation (FFT) of this additional set of reflections (red in (d)) indicates that it can be assigned to the surface layer.

on the heterogeneity of molecular behavior.^{34–37} With SMS subpopulations, rare events and the influence of structural heterogeneous environment on the different single particles can be revealed. However, detailed structural analysis of the nanowires and nanoclusters is hindered due to the limited spatial resolution.

Here, we investigated silver nanowires using a combination of SMS and transmission electron microscopy (TEM) including analytical techniques. Using wide-field illumination, we observed synchronous fluorescence emission from emitters located at distinct positions along single nanowires. By correlating fluorescence, high-resolution TEM, and energy-dispersive X-ray spectroscopy, we were able to attribute the cooperative behavior to spectroscopic features of the silver nanowires.

RESULTS AND DISCUSSION

Single crystalline silver nanowires, synthesized by a seedless wet-chemical approach (Materials and Methods), were imaged using bright-field electron microscopy (Materials and Methods). The image of an exemplary silver nanowire (Ag-NW) in Figure 1a shows an $\sim 11 \mu\text{m}$ long and 80 nm thick Ag-NW deposited on a holey carbon-coated copper grid. As can be seen, the nanowire has a rather homogeneous thickness over the entire length.

Higher magnification images and diffraction studies revealed more detailed information of the Ag-NWs structure. Figure 1b shows a higher magnification bright-field image of a selected region of this Ag-NW (indicated by the red square in Figure 1a). A 10–20 nm thick layer surrounding the Ag-NW can be observed, which is attributed to the sodium citrate used for the growth and stabilization of the Ag-NWs during their synthesis (Materials and Methods). Additionally, particles of about 5–10 nm in size can be seen in this citrate layer. The electron diffraction pattern (Figure 1b inset) taken in the middle of the Ag-NW from Figure 1b displays spots corresponding to Ag reflections. In addition, reflections due to twinning, that is, two or more separate crystals sharing some of the same crystal lattice points in a symmetrical manner, of the Ag-NW occur in accordance with the observations reported in the literature where five-fold twinning is frequently observed for Ag-NWs and nanoparticles.^{38,39} Moreover, diffraction experiments and fast Fourier transformation (FFT) analysis of high-resolution TEM (HRTEM) micrograph analysis taken at various positions along the surface of the Ag-NW and of particles in the citrate layer showed additional weaker reflections attributed to silver oxide. Hence, the particles in the citrate layers are primarily pure Ag particles, and only some of them are composed of silver oxide.

When imaged at a higher magnification, an additional ~ 1 nm thick layer is observed at the interface between the NW and citrate layer, consisting of 2–3 atomic layers (Figure 1c). The FFT of the marked area (red) from Figure 1c indicates reflections corresponding to the d values of Ag and shows the same orientation as the nanowire in [011] (Figure 1d). Furthermore, one additional set of reflections was found (marked red in Figure 1d), which corresponds either to the $(-1-11)$ plane of Ag_2O or to the (-111) of AgO. By comparing the inverse FFT of these reflections to the original image, it becomes clear that these reflections stem from the surface layer (Figure 1e). Thus, the Ag-NWs possess a thin silver oxide layer, in accordance with data from additional diffraction experiments and FFT analysis (data not shown).

In order to unravel the optical properties of the Ag-NWs, the luminescence of individual NWs was investigated using a wide-field optical microscope with single molecule fluorescence sensitivity (Materials and Methods). Typically each NW had several localized spots from where luminescence emission occurred. Single particle tracking (SPT) was used to determine the positions of these emitting entities on the silver nanowires by fitting, frame-by-frame, a two-dimensional Gaussian function to the fluorescence spots:

$$I = A_0 \exp\left(-\frac{(x-x_0)^2}{2\sigma^2}\right) \exp\left(-\frac{(y-y_0)^2}{2\sigma^2}\right) \quad (1)$$

where A_0 and σ^2 are the amplitude and the variance of the two-dimensional Gaussian curve, respectively, and x_0 and y_0 are the coordinates of the position of the individual emitting entities. With this method, the positions of the entities can be determined with a positioning accuracy of up to 5 nm (on glass substrates) depending on the signal-to-noise ratio. Changes in the brightness of the emitting entities, background fluorescence, or other emitters nearby can decrease the signal-to-noise ratio and thereby the positioning accuracy. For experiments requiring an overlay of TEM and fluorescence images, a Si_3N_4 membrane was used as a substrate (Materials and Methods). This resulted in a reduced signal-to-noise ratio and thus a lower positioning accuracy (typically about 20–25 nm) as compared to experiments on glass substrates, which were only used for fluorescence measurements.

The fluorescence from the spots was not continuous, but blinking and changes in fluorescence intensity was observed (Figure 2). This effect has been reported previously using confocal microscopy²³ and was attributed to random surface diffusion and agglomeration of Ag atoms which form photoactive Ag nanoclusters⁴⁰ or photoactivated silver oxide.²² Interestingly, using the wide-field excitation, we find that oftentimes the emission from several spots on a single NW is highly cooperative; that is, blinking and intensity

fluctuations are observed exactly at the same time, given our time resolution of 10 ms. Blinking of both cooperatively emitting sites, as well as that of single emitters, follows a power law (see experimental data in Figure S1 in the Supporting Information). As an example of the cooperative effect, Figure 2 displays three consecutive frames extracted from a sequence of images (movie S1 in Supporting Information) showing the synchronous appearance and disappearance of two spatially separated fluorescence spots along a single Ag-NW (the approximate shape of the nanowire as observed using bright-field microscopy (data not shown) is indicated by the yellow striped line). The fluorescence patterns of the spots were fitted with two-dimensional Gaussian functions (eq 1). The two centers of emission (marked by arrows in Figure 2a,b) were separated by a distance of about $1.5 \mu\text{m}$. The recorded trajectories of the fluorescence intensity of both emitters show repetitive correlated blinking events (Figure 2c). The time at which emission occurs appears to be stochastic, but the fluorescence emission from both emitters is perfectly synchronized (as indicated by the gray dotted lines). Additionally, a statistical analysis of 120 distances between pairs of synchronous emitters was performed. The distribution of these distances (Figure S2 in the Supporting Information) is continuous and decays with longer distances. This observation can be explained by the exponential decay of the intensity of surface plasmons along metal surfaces. This plasmon damping is caused by power loss in the metal. Moreover, while the exemplary trace from Figure 2 shows rather long on-times, oftentimes observed on-times were below our time resolution of 10 ms; that is, we observed only a single “on-frame”.

In our experiments, we investigated more than 200 nanowires and detected cooperative emission for about 35% of the nanowires, and about 2% of the NWs exhibited no emission at all while the remaining NWs showed noncoupled blinking of single emission sites. Interestingly, cooperative emission was observed only after an aging time under air atmosphere of at least one day (after growth); we never observed cooperative emission from freshly prepared nanowires. Also, the total number of emitters increased with aging. This indicates that the formation of silver clusters from silver oxide layers is a prerequisite for the occurrence of the observed cooperative emission. Furthermore, emitters on different NWs were never observed to emit simultaneously even when they were at distances smaller than the largest distances (approximately $10 \mu\text{m}$) for which the cooperative effect was observed (data not shown). Thus the coupling of the emitters observed through the cooperative emission occurs *via* the Ag-NW most likely through surface plasmons.

The question then arises whether the two (or more) cooperative emissive sites are all active or whether

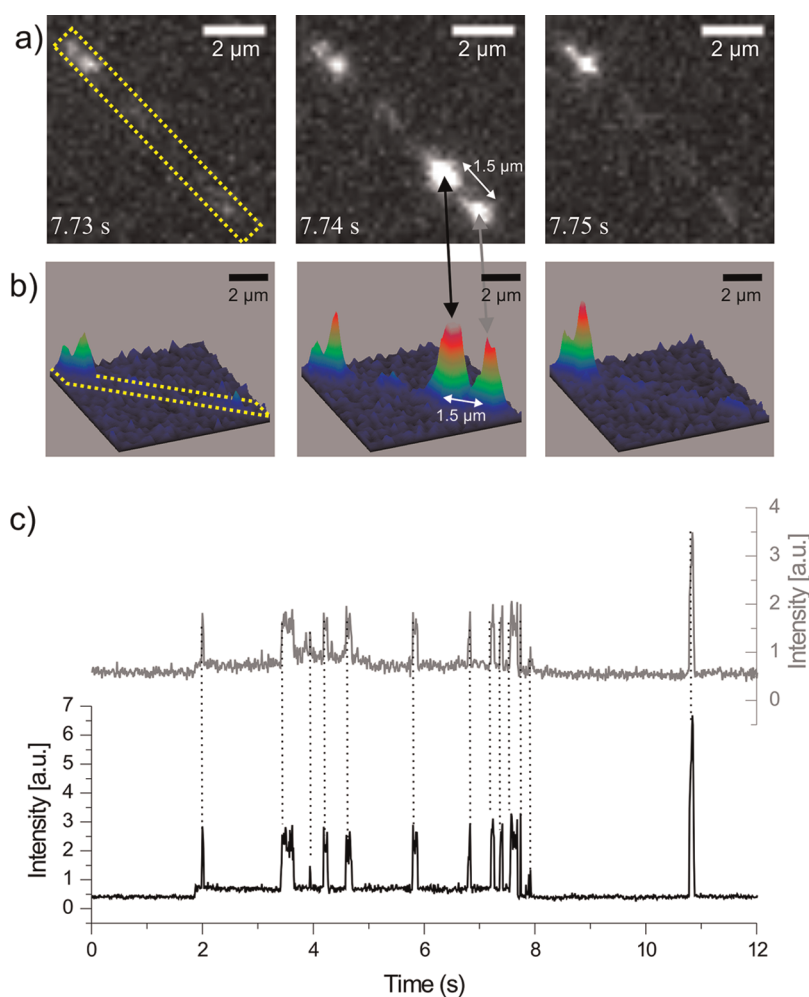


Figure 2. Wide-field fluorescence study of a Ag-NW. (a) Series of wide-field images of emitting entities exhibiting a cooperative fluorescence emission. The positions of the emitters are marked with a black and gray arrow in the middle panel. (b) Corresponding 3D surface plots of the fluorescence intensity. (c) Fluorescence intensity trajectories over time for both emitters (gray and black lines matching the color of the respective arrows in (a)). Exemplary synchronous emission events are highlighted by dashed lines.

some of them behave in a passive fashion (*i.e.*, as scatterers). In the case of one active center, the laser beam would excite one entity which could emit itself but also couple energy to the surface plasmon of the nanowire. This energy could then be transmitted to a passive center (such as a defect site or a nanoparticle), located on the same wire, but separated by some distance. In this case, the emitted fluorescence intensity of all emissive sites should be perfectly correlated. In contrast, we observed for NWs showing more than two coupled emitters, such as the example in Figure 3a (movie S2 in Supporting Information), that while the emission off all emission sites is highly cooperative at times (Figure 3b), there are also emission bursts from only subsets of the emitters (Figure 3c). Therefore, it is highly likely that these emitters are active centers rather than passive scatterers.

In order to provide direct evidence that cooperative emitters are active and not passive scattering centers, we performed additional experiments in which we

temporarily blocked the excitation of single emitters by inserting a physical mask in the excitation pathway, while at the same time always collecting the emission from all emitters. In the case of scattering (*i.e.*, passive emitters), one would still expect to see cooperative emission. However, if there is more than one active center involved, then one will observe emission only at the excited sites and no signal from the sites that are blocked. The results of an exemplary experiment are shown in Figure 4. A single Ag-NW showing cooperative emission from several sites when using wide-field illumination (Figure 4a and movie S3a in the Supporting Information) is shown. If the excitation of either emissive site is physically masked, no fluorescence from it is observed, while the other sites still show emission (Figure 4b,c and movie S3b,c in the Supporting Information). After removing the aperture, the Ag-NW shows again cooperative fluorescence emission (Figure 4d and movie S3d in the Supporting Information) and thus the emissive centers are active rather than passive scatterers.

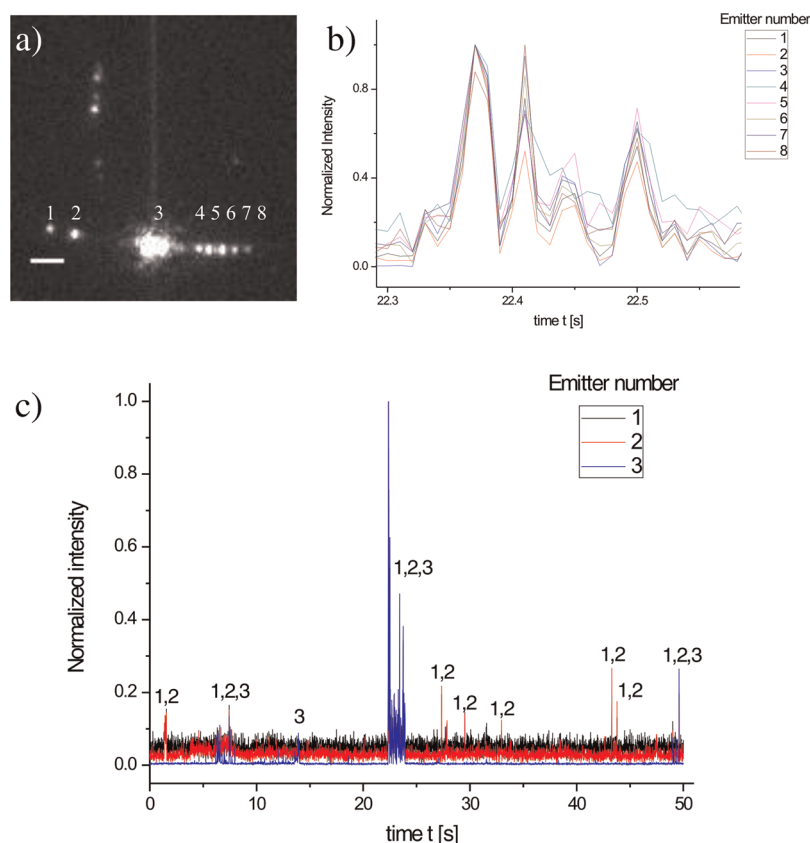


Figure 3. Selected wide-field fluorescence image of movie S2 showing cooperative emission from eight emitters on one single nanowire (scale bar is 2 μm). The computed Pearson's correlation coefficients are given in Table S2. (b) Time trajectory of emitted fluorescence intensity from the eight emission sites showing highly correlated intensity fluctuations. The displayed data are only a small fraction of the complete time trajectory. (c) Complete fluorescence time trajectories of cooperative emission from the NW shown in (a). For clarity, only emitters 1, 2, and 3 are displayed. These three emitters exhibit at some times cooperative fluorescence bursts (marked by respective numbers above the trajectory); however, there are also burst events from only two emitters or even from only a single emitter.

To unravel structural and chemical reasons for the occurrence of the cooperative effect, we imaged a nanowire by TEM, for which the cooperative effect was observed in the wide-field fluorescence measurements. The TEM image (Figure 5a) shows a 1.38 μm long and 80 nm thick Ag-NW surrounded by several small particles. The NW and the nanoparticles were characterized with energy-dispersive X-ray spectroscopy (EDX) measurements in scanning transmission electron microscopy (STEM) mode in detail to correlate optical and chemical properties (Table S1).

To find out which parts of the nanowire cause the emission, approximately 50 EDX measurements were performed at different parts of the nanowire and surrounding nanoparticles using an electron beam size of about 1 nm. Figure 5a shows the bright-field image of the Ag-NW together with numbers indicating the positions of the EDX measurements. The values of the quantification of the EDX spectra are given in Table S1 (Supporting Information). Besides Ag, which was detected at all positions along the nanowire, also O (red numbers) and some traces of S (yellow numbers) were found. The O stems most likely from the thin surface layer described above. The FFT taken from a part of the

surface of the Ag-NW (Figure 5b) shows reflections of Ag (reflections marked in white) and silver oxide (reflections marked in red). Both the diffraction as well as the FFT data show that most of the particles investigated by EDX contain mainly Ag, and some have a high O content, supporting the presence of silver oxide (e.g., positions 13, 14, 17, 42, 22, 25, 30, and 31). In addition, S, probably originating from air, is detected in parts of the citrate film and in some of the nanoparticles (EDX measurements 5, 6, 7, 14, 21–25, 32, 33, 35, 39, 40, 47, and 48).

The 3D surface plots of the fluorescence intensity (Figure 5c) for five frames extracted from a wide-field fluorescence movie (movie S4 in Supporting Information) show the coupling of the fluorescence emission between two entities along the nanowire (as imaged by TEM). The corresponding fluorescence intensity time trajectories are depicted in Figure 5d (gray and black curves corresponding to the left and right fluorescent spot, respectively). Both appear simultaneously (i.e., within less than 10 ms, the experimental time resolution) at about 7.8 s and disappear simultaneously at about 9.2 s. Between, strong fluorescence intensity fluctuations are detected, which also appear

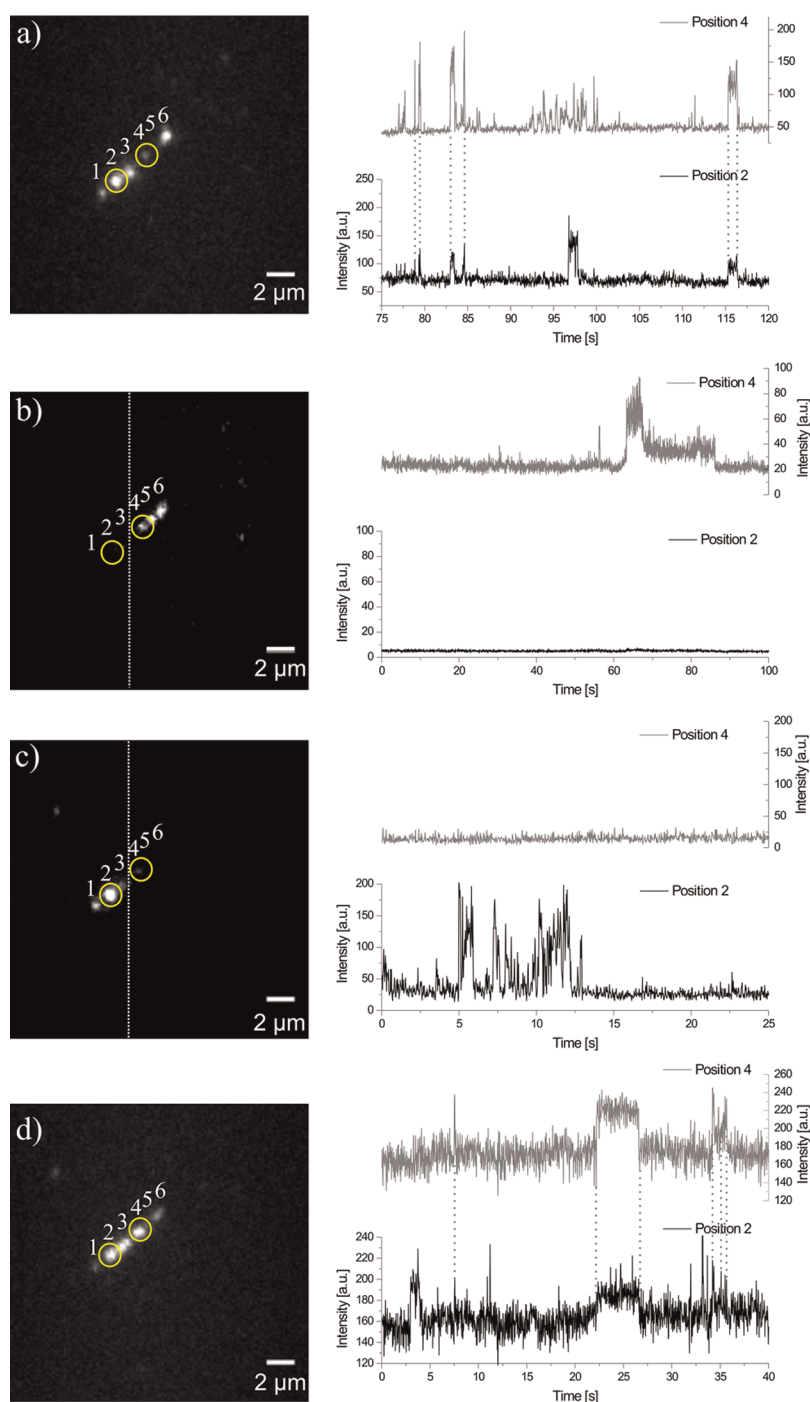


Figure 4. Wide-field fluorescence study of two active emitting entities on a Ag-NW. (a) Wide-field image with fluorescence time trajectories for two emitters (positions 2 and 4, marked with yellow circles) exhibiting cooperative fluorescence emission. Using an aperture in the excitation laser pathway from the left (b) or from the right side of the white dotted line (c), only one of these emitters is excited, respectively. Emitters, which are not excited, show no fluorescence emission. (d) Wide-field image and time trajectory taken after the mask has been removed show again cooperative fluorescence emission from positions 2 and 4.

to be synchronized, as highlighted by the dotted line between exemplary simultaneous fluorescence burst events. After 9.6 s, the signals appear again before the measurement stops. For each frame, the determined positions of the two emitters are plotted in Figure 5e (gray and black). The average distance between the two cooperative emitters was found to be 911 ± 49 nm.

As the length of this nanowire is $1.38 \mu\text{m}$ (as determined by TEM), the two emitters are not located at the ends of the NW. However, by inspecting the “map” of the EDX measurements displayed in Figure 5a, we were able to identify two regions with high O content (red numbers) separated by about 900 nm (highlighted with the gray and black dotted

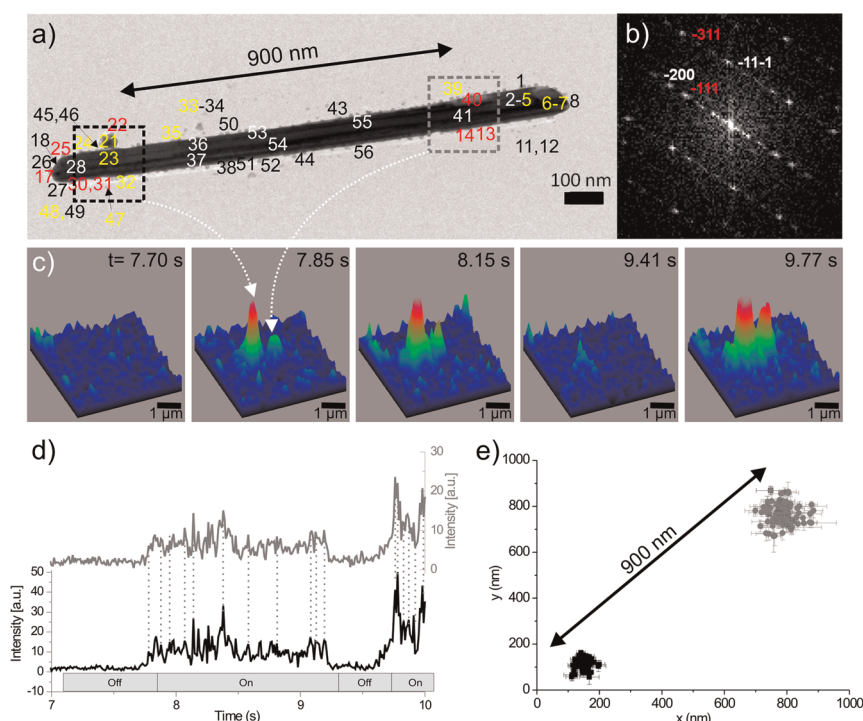


Figure 5. (a) Bright-field TEM image of a Ag-NW, showing cooperative fluorescence emission. The position investigated by EDX measurements (data shown in Supporting Information Table S1) is marked with numbers (black/white numbers show high Ag values; red numbers contain high Ag and high O values; yellow numbers contain high Ag and high S values). (b) FFT taken from a part of the surface indicates reflections of Ag (marked white) and Ag₂O (marked red) and shows an orientation in [001]. (c) Snapshots of the fluorescence intensity distribution emitted from the same NW displayed by 3D surface plots. The cooperative emission from two spots is marked by arrows. (d) Fluorescence time trajectories of both emitters showing interesting fluctuations of the cooperative effect (marked with dashed lines). (e) Determined positions with corresponding error bars (on average 15 nm (black) and 32 nm (gray)) for both emitters.

squares). This observation and the necessity for sample aging in the presence of oxygen for synchronous emission mentioned strongly suggest that one can attribute cooperative emitters to silver clusters which are generated photochemically from silver oxide^{30–33} and which are optically coupled through the silver nanowire.

Additional support for the interpretation that the coupled emitters are silver clusters generated photochemically from silver oxide comes from the following observations: TEM studies showed that there is a 2–3 atomic layer thin silver oxide layer around the silver nanowires. During the TEM measurements, it could be observed that exposure of the sample to the electron beam over long time scales damages the citrate layer around the nanowires and also the silver oxide layer. Fluorescence measurements performed

directly afterward showed no fluorescence of previously emitting nanowires. Additionally, EDX studies showed that some nanowires, which did not exhibit any fluorescence emission, contained a relatively high amount of sulfide, which might prevent the formation of a silver oxide layer and thus the generation of a silver cluster.

CONCLUSIONS

In summary, while emission of single entities on silver nanostructures is well studied, we observed a coupled emission for some of the investigated NWs (about 35%). Such a coupled emission can only be observed if several active emitters are investigated simultaneously. Since the emitters are located within a few micrometers on the NW, the coupled emission can be attributed to plasmonic coupling through the wire.

MATERIALS AND METHODS

Crystalline Ag-NWs were synthesized using a seedless, surfactantless wet-chemical fabrication developed by Caswell *et al.*²⁹ This solution, containing about 100 nm thick and up to 15 μm long Ag-NWs, was then spin-coated onto a glass cover slide (20 mm × 20 mm, thickness 170 μm, Marienfeld). Fluorescence signals from individual nanowires were then collected using a wide-field setup described previously.⁴¹ Briefly, an

Eclipse TE200 (Nikon) epi-fluorescence microscope with a high numerical aperture (NA) oil-immersion objective (Nikon Plan Apo 100×, NA = 1.40) was used, and the nanowires were excited at 633 nm with a He–Ne gas laser with an excitation power of 7 mW (measured in front of the microscope). Fluorescence was collected using a combination of filters (dichroic mirror 640 nm cutoff and band-pass 730/140 AHF) and imaged onto a back-illuminated electron multiplying charge-coupled device

(EM-CCD) camera (Andor, iXon DV897). A series of typically 1000 fluorescence images were recorded with a temporal resolution of 10 ms per frame.

In some experiments, we wanted to selectively excite only parts of a Ag-NW. We therefore placed a physical aperture in the excitation laser pathway in front of the microscope to shrink the excited area, while keeping the complete detection area.

To combine optical and structural properties, we also performed experiments for which Ag-NWs were deposited on silicon nitride membranes (Si_3N_4 , Agar Scientific). For these samples, a different objective lens (Nikon water immersion objective, NA = 1.20, $63\times$) was used. Some of the optically investigated nanowires were then also studied by TEM in order to correlate fluorescence and structural features. These investigations were done using a FEI Titan 80-300 (S)TEM microscope equipped with a Gatan Tridiem image filter and an EDAX energy-dispersive X-ray spectroscopy detector for analytical measurements. The Titan was operated with 300 kV. A high-angle annular dark-field (HAADF) detector from Fischione Instruments (model 3000) was attached to the microscope for scanning TEM imaging.

Besides the correlative optical and TEM measurements, some Ag-NWs were also investigated only using the TEM measurements, and for these measurements, samples were prepared by placing the Ag-NW on a carbon-coated copper grid (Plano).

Conflict of Interest: The authors declare no competing financial interest.

Acknowledgment. Financial support from DFG-SFB 749 and the cluster of excellence Nanosystems Initiative Munich (NIM) is gratefully acknowledged. The authors also thank C. Hohmann for TOC graphics design.

Supporting Information Available: Description of supporting movies, additional figures and tables. This material is available free of charge via the Internet at <http://pubs.acs.org>.

REFERENCES AND NOTES

- Barnes, W. L.; Dereux, A.; Ebbesen, T. W. Surface Plasmon Subwavelength Optics. *Nature* **2003**, *424*, 824–830.
- Ozbay, E. Plasmonics: Merging Photonics and Electronics at Nanoscale Dimensions. *Science* **2006**, *311*, 189–193.
- Kolesov, R.; Grotz, B.; Balasubramanian, G.; Stohr, R. J.; Nicolet, A. A. L.; Hemmer, P. R.; Jelezko, F.; Wrachtrup, J. Wave-Particle Duality of Single Surface Plasmon Polaritons. *Nat. Phys.* **2009**, *5*, 470–474.
- Novotny, L. Effective Wavelength Scaling for Optical Antennas. *Phys. Rev. Lett.* **2007**, *98*.
- Mohanty, P.; Yoon, I.; Kang, T.; Seo, K.; Varadwaj, K. S. K.; Choi, W.; Park, Q. H.; Ahn, J. P.; Suh, Y. D.; Ihee, H.; *et al.* Simple Vapor-Phase Synthesis of Single-Crystalline Ag Nanowires and Single-Nanowire Surface-Enhanced Raman Scattering. *J. Am. Chem. Soc.* **2007**, *129*, 9576–9577.
- Baik, J. M.; Lee, S. J.; Moskovits, M. Polarized Surface-Enhanced Raman Spectroscopy from Molecules Adsorbed in Nano-Gaps Produced by Electromigration in Silver Nanowires. *Nano Lett.* **2009**, *9*, 672–676.
- Fang, Y. R.; Wei, H.; Hao, F.; Nordlander, P.; Xu, H. X. Remote-Excitation Surface-Enhanced Raman Scattering Using Propagating Ag Nanowire Plasmons. *Nano Lett.* **2009**, *9*, 2049–2053.
- Yoon, I.; Kang, T.; Choi, W.; Kim, J.; Yoo, Y.; Joo, S. W.; Park, Q. H.; Ihee, H.; Kim, B. Single Nanowire on a Film as an Efficient SERS-Active Platform. *J. Am. Chem. Soc.* **2009**, *131*, 758–762.
- Ashley, J. C.; Emerson, L. C. Dispersion-Relations for Non-radiative Surface Plasmons on Cylinders. *Surf. Sci.* **1974**, *41*, 615–618.
- Takahara, J.; Yamagishi, S.; Taki, H.; Morimoto, A.; Kobayashi, T. Guiding of a One-Dimensional Optical Beam with Nanometer Diameter. *Opt. Lett.* **1997**, *22*, 475–477.
- Weeber, J. C.; Dereux, A.; Girard, C.; Krenn, J. R.; Goudonnet, J. P. Plasmon Polaritons of Metallic Nanowires for Controlling Submicron Propagation of Light. *Phys. Rev. B* **1999**, *60*, 9061–9068.
- Dickson, R. M.; Lyon, L. A. Unidirectional Plasmon Propagation in Metallic Nanowires. *J. Phys. Chem. B* **2000**, *104*, 6095–6098.
- Krenn, J. R.; Lamprecht, B.; Ditlbacher, H.; Schider, G.; Salerno, M.; Leitner, A.; Aussenegg, F. R. Non Diffraction-Limited Light Transport by Gold Nanowires. *Europhys. Lett.* **2002**, *60*, 663–669.
- Murray, B. J.; Li, Q.; Newberg, J. T.; Hemminger, J. C.; Penner, R. M. Silver Oxide Microwires: Electrodeposition and Observation of Reversible Resistance Modulation upon Exposure to Ammonia Vapor. *Chem. Mater.* **2005**, *17*, 6611–6618.
- Brunker, S. E.; Cederquist, K. B.; Keating, C. D. Metallic Barcodes for Multiplexed Bioassays. *Nanomedicine* **2007**, *2*, 695–710.
- Pan, S. L.; Rothberg, L. J. Enhancement of Platinum Octaethyl Porphyrin Phosphorescence near Nanotextured Silver Surfaces. *J. Am. Chem. Soc.* **2005**, *127*, 6087–6094.
- Pan, S. L.; Wang, Z. J.; Rothberg, L. J. Enhancement of Adsorbed Dye Monolayer Fluorescence by a Silver Nanoparticle Overlay. *J. Phys. Chem. B* **2006**, *110*, 17383–17387.
- Guo, S. H.; Britti, D. G.; Heetderks, J. J.; Kan, H. C.; Phaneuf, R. J. Spacer Layer Effect in Fluorescence Enhancement from Silver Nanowires over a Silver Film; Switching of Optimum Polarization. *Nano Lett.* **2009**, *9*, 2666–2670.
- Akimov, A. V.; Mukherjee, A.; Yu, C. L.; Chang, D. E.; Zibrov, A. S.; Hemmer, P. R.; Park, H.; Lukin, M. D. Generation of Single Optical Plasmons in Metallic Nanowires Coupled to Quantum Dots. *Nature* **2007**, *450*, 402–406.
- Grillet, C.; Monat, C.; Smith, C. L. C.; Eggleton, B. J.; Moss, D. J.; Frederick, S.; Dalacu, D.; Poole, P. J.; Lapointe, J.; Aers, G.; *et al.* Nanowire Coupling to Photonic Crystal Nanocavities for Single Photon Sources. *Opt. Express* **2007**, *15*, 1267–1276.
- Fang, Z. Y.; Fan, L. R.; Lin, C. F.; Zhang, D.; Meixner, A. J.; Zhu, X. Plasmonic Coupling of Bow Tie Antennas with Ag Nanowire. *Nano Lett.* **2011**, *11*, 1676–1680.
- Peysner, L. A.; Vinson, A. E.; Bartko, A. P.; Dickson, R. M. Photoactivated Fluorescence from Individual Silver Nanoclusters. *Science* **2001**, *291*, 103–106.
- Clayton, D. A.; Benoist, D. M.; Zhu, Y.; Pan, S. L. Photoluminescence and Spectroelectrochemistry of Single Ag Nanowires. *ACS Nano* **2010**, *4*, 2363–2373.
- Wild, B.; Cao, L.; Sun, Y.; Khanal, B. P.; Zubarev, E. R.; Gray, S. K.; Scherer, N. F.; Pelton, M. Propagation Lengths and Group Velocities of Plasmons in Chemically Synthesized Gold and Silver Nanowires. *ACS Nano* **2012**, *6*, 472–482.
- Zong, R. L.; Zhou, J.; Li, Q.; Du, B.; Li, B.; Fu, M.; Qi, X. W.; Li, L. T.; Buddhudu, S. Synthesis and Optical Properties of Silver Nanowire Arrays Embedded in Anodic Alumina Membrane. *J. Phys. Chem. B* **2004**, *108*, 16713–16716.
- Jana, N. R.; Gearheart, L.; Murphy, C. J. Wet Chemical Synthesis of Silver Nanorods and Nanowires of Controllable Aspect Ratio. *Chem. Commun.* **2001**, 617–618.
- Sun, Y. G.; Gates, B.; Mayers, B.; Xia, Y. N. Crystalline Silver Nanowires by Soft Solution Processing. *Nano Lett.* **2002**, *2*, 165–168.
- Wiley, B.; Sun, Y. G.; Xia, Y. N. Synthesis of Silver Nanostructures with Controlled Shapes and Properties. *Acc. Chem. Res.* **2007**, *40*, 1067–1076.
- Caswell, K. K.; Bender, C. M.; Murphy, C. J. Seedless, Surfactantless Wet Chemical Synthesis of Silver Nanowires. *Nano Lett.* **2003**, *3*, 667–669.
- Kötz, R.; Yeager, E. Raman Studies of the Silver/Silver Oxide Electrode. *J. Electroanal. Chem.* **1980**, *111*, 105–110.
- Watanabe, T.; Kawanami, O.; Honda, K.; Pettinger, B. Evidence for Surface Ag^+ Complexes as the SERS-Active Sites on Ag Electrodes. *Chem. Phys. Lett.* **1983**, *102*, 565–570.
- Brandt, E. S. Selective Enhanced Raman-Scattering from an Oxacarboxyanine Dye and 1-Phenyl-5-mercaptopotetrazole Adsorbed to Silver and Silver-Halide Surfaces in Photographic Films. *Appl. Spectrosc.* **1993**, *47*, 85–93.

33. Wang, X.; Wen, H.; He, T. J.; Zuo, J.; Xu, C. Y.; Liu, F. C. Enhancement Mechanism of Sers from Cyanine Dyes Adsorbed on Ag₂O Colloids. *Spectrochim. Acta, Part A* **1997**, *53*, 2495–2504.
34. Xie, X. S. Single-Molecule Spectroscopy and Dynamics at Room Temperature. *Acc. Chem. Res.* **1996**, *29*, 598–606.
35. Dickson, R. M.; Cubitt, A. B.; Tsien, R. Y.; Moerner, W. E. On/Off Blinking and Switching Behaviour of Single Molecules of Green Fluorescent Protein. *Nature* **1997**, *388*, 355–358.
36. Bartko, A. P.; Dickson, R. M. Imaging Three-Dimensional Single Molecule Orientations. *J. Phys. Chem. B* **1999**, *103*, 11237–11241.
37. Moerner, W. E.; Orrit, M. Illuminating Single Molecules in Condensed Matter. *Science* **1999**, *283*, 1670–1676.
38. Chen, H.; Gao, Y.; Zhang, H.; Liu, L.; Yu, H.; Tian, H.; Xie, S.; Li, J. Transmission-Electron-Microscopy Study on Fivefold Twinned Silver Nanorods. *J. Phys. Chem. B* **2004**, *108*, 12038–12043.
39. Damm, C.; Segets, D.; Yang, G.; Vieweg, B. F.; Spiecker, E.; Peukert, W. Shape Transformation Mechanism of Silver Nanorods in Aqueous Solution. *Small* **2011**, *7*, 147–156.
40. Wu, X. Y.; Yeow, E. K. L. Fluorescence Blinking Dynamics of Silver Nanoparticle and Silver Nanorod Films. *Nanotechnology* **2008**, *19*, 035706.
41. Kirstein, J.; Platschek, B.; Jung, C.; Brown, R.; Bein, T.; Brauchle, C. Exploration of Nanostructured Channel Systems with Single-Molecule Probes. *Nat. Mater.* **2007**, *6*, 303–310.